Exploring the Early Steps of Amyloid Peptide Aggregation by Computers

NORMAND MOUSSEAU† AND PHILIPPE DERREUMAUX*,‡

Département de Physique and Regroupement Québécois sur les Matériaux de Pointe, Université de Montréal, C.P. 6128, Succursale Centre-ville, Montréal, Québec, Canada, and Laboratoire de Biochimie Théorique, UPR 9080 CNRS, Institut de Biologie Physico-Chimique et Université Paris 7, 13 rue Pierre et Marie Curie, 75005 Paris, France

Received April 13, 2005

ABSTRACT

The assembly of normally soluble proteins into amyloid fibrils is a hallmark of neurodegenerative diseases. Because protein aggregation is very complex, involving a variety of oligomeric metastable intermediates, the detailed aggregation paths and structural characterization of the intermediates remain to be determined. Yet, there is strong evidence that these oligomers, which form early in the process of fibrillogenesis, are cytotoxic. In this paper, we review our current understanding of the underlying factors that promote the aggregation of peptides into amyloid fibrils. We focus here on the structural and dynamic aspects of the aggregation as observed in state-of-the-art computer simulations of amyloid-forming peptides with an emphasis on the activation−relaxation technique.

1. Introduction

The deposition of amyloid fibrils is a hallmark of many types of human disease.[1,2] For example, Alzheimer's disease results from the accumulation of the amyloid β-protein (Aβ) present in two forms, 40 (Aβ_{1-40}) and 42 (Aβ_{1-42}) amino acids, produced through endoproteolysis of the β-amyloid precursor transmembrane protein. Similarly, transmissible spongiform encephalopathies involve the prion protein (PrP) of 240 amino acids; 80% of human prion diseases are sporadic with the modes of natural transmission remaining undetermined, and about 15% are inherited (familial forms of Creutzfeld−Jakob disease, fatal familial insomnia, and Gerstmann−Straussler syndrome) by mutations in the human prion gene within chromosome 20.[3] Interestingly, several proteins such as myoglobin or lysozyme, which normally do not give rise to amyloid, can also be converted to fibrils under denaturing conditions.[2]

Although these proteins have very different amino acid sequences and biophysical properties in solution (PrP is α-helical but Aβ is disordered), they all aggregate into a common cross-β-sheet structure with the β-strands perpendicular to the fiber axis.[4,5] Because amyloid fibrils are insoluble and do not form crystals, high-resolution atomic structures are still lacking and our undertanding of fibril structure and stability comes essentially from X-ray fibril diffraction, negative stain electron microscopy, atomic force spectroscopy, and, more recently, solid-state nuclear magnetic resonance (NMR) spectroscopy.

There is mounting evidence that the toxicity of these fatal neurodegenerative diseases may also be caused by the soluble intermediate oligomers in addition to the mature fibrils.[6,7] It is therefore important to characterize the early steps of oligomer formation at the atomic level. Because these structures are metastable and short-lived, experimental data are difficult to obtain.[5,8] Moreover, protein aggregation is very complex, involving a variety of morphologies and different oligomeric intermediates, and it depends closely on the experimental conditions such as pH and ionic strength.

The ease with which oligomers grow is likely determined by the size of their critical nucleus, which determines the point at which half the oligomers will form a fiber. This critical size is also sequence-dependent within the nucleation−growth kinetic model. With use of a photoinduced cross-linker coupled to size-exclusion chromatography, Aβ_{1-40} is found to exist as a mixture of monomers, dimers, trimers, and tetramers in rapid equilibrium, while Aβ_{1-42} forms pentamer/hexamer units. Once these critical units or nuclei of highest free energy are formed, the aggregation proceeds rapidly into amyloid fibers.[8] The lag phase, in which no aggregation is observed, can be overcome by the presence of prefibrillar states or metal ions.

Predicting the aggregation paths and the detailed atomic structures of the intermediates is a difficult task for computer simulations. The lag phase for Aβ_{1-40} takes several days and thus is several orders of magnitude in time beyond what can be obtained by current all-atom simulations. It is also difficult to determine the minimal model that reproduces the essential structural and energetic features of peptides and allows an extensive search of conformational space. A variety of chain representation and energy models and methods including molecular dynamics (MD), discontinuous MD, replica exchange MD simulations, and Monte Carlo-based methods (MC) have been applied to amyloid-forming peptides.

The goal of this Account is to present our current understanding of the atomistic details of the self-assembly and growth processes of small amyloid-forming peptides in the context of recent computer simulations and experimental data. To this end, we present the results of activation−relaxation technique (ART) simulations coupled

Normand Mousseau received B.Sc. and M.Sc. degrees from Université de Montréal and his Ph.D. degree from Michigan State University. He was a postdoctoral fellow at Oxford University and Université de Montréal and then became an assistant professor of physics at Ohio University. In June 2001, he moved to Université de Montréal where he is now an associate professor and the Canada Research Chair in Computational Physics of Complex Materials.

Philippe Derreumaux received his Ph.D degree from Lille University. Following researcher positions at the CNRS Chemistry department in Lille and Paris and at New York University from 1989 to 1999, he was professor at the biology department of Marseille University. Since 2003, he has been professor of bioinformatics at University of Paris 7.

† Université de Montréal.
‡ Institut de Biologie Physico-Chimique et Université Paris 7.

10.1021/ar050045a CCC: $30.25
Published on Web 09/17/2005

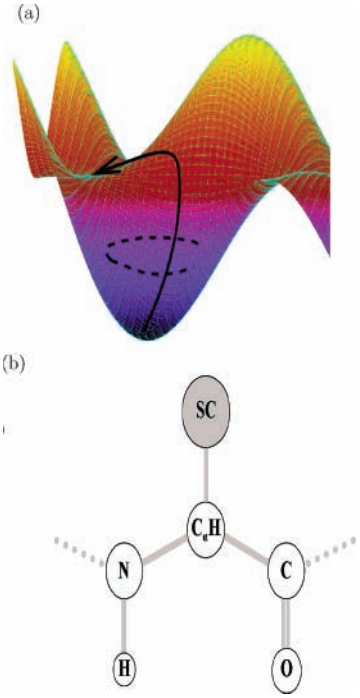

FIGURE 1. Schematic representation of the activation step of ART. The surface represents the energy landscape. Starting from a local minimum, the conformation is pushed in a random direction (represented by the solid line) until it leaves the harmonic well (border indicated by a dashed line). The conformation is then pushed along a direction of negative curvature until it reaches a saddle point. Panel b shows the protein model. Each amino acid is described by five main-chain atoms plus a bead, indicated by the letter "Sc", which represents the side chain.

with a coarse-grained energy model (OPEP) on peptides of different sizes and sequences. These include the Aβ fragment spanning residues 16−22 (Aβ_{16-22}) in dimeric[9] and trimeric[10] forms and the KFFE and KPGE tetrapeptides ranging from tetramers to octamers.[11−13] Aβ_{16-22} of sequence KLVFFAE was chosen because it is known to form fibrils with antiparallel orientations of the chains by NMR solid-state analysis at neutral pH[14] and comprises the central hydrophobic core that is thought to be important in full-length Aβ assembly. KFFE is the shortest peptide to form amyloid fibrils similar to those built from large proteins,[15] while KPGE is expected to be random coil.

2. Simulation Approaches

2.1. Activation−Relaxation Technique. Since the aggregation process extends over a time scale much beyond a microsecond, it is not possible to use standard MD simulations in explicit solvent.[16] Exploiting the implicit solvent incorporated into the interaction potential, we turn instead to the activation−relaxation technique (ART), a method[17,18] that focuses on identifying the activated pathway going from one local minimum conformation to a neighboring one.

More specifically, we use ART nouveau,[18] which goes as follows (see Figure 1A): (1) Starting from a local energy minimum, we slowly apply a random deformation to bring the conformation outside the harmonic region surrounding the local minimum. In practice, the conformation is deformed until the direction of smallest curvature on the energy surface falls below a negative threshold, indicating the existence of a transition point in the vicinity. The details of this procedure can be adapted to any specific problem. For example, it is possible to restrict the initial move to one fragment or to a section of a protein. Moreover, selecting the direction of lowest curvature at this stage recovers the normal-mode approach. (2) The conformation is then pushed along the eigen direction corresponding to the negative curvature, while the energy is minimized in the perpendicular hyperplane, converging onto a transition point with any desired accuracy. Taken together, these two steps represent the *activation*. (3) From the transition state, the conformation is pushed into a new basin, and the energy is minimized until the total force approaches zero. This constitutes the *relaxation* phase. Taken together, these two steps generate what is called *an event*. We emphasize that the events are physically based because they connect two touching basins through a well-defined transition point. The move to the new minimum is accepted using the Metropolis criterion: $P_{\text{accept}} = e^{-\Delta E/(k_B T)}$, ΔE being the energy difference between the two minima and $k_B T$ the product of Boltzmann's constant and temperature.

ART nouveau has been extensively characterized in amorphous semiconductors and Lennard-Jones clusters[18] as well as proteins.[19] It differs from real-space MC and standard MD simulations in two respects. First, ART events are defined directly in the space of conformations, so it can generate moves of any complexity, in contrast with real-space MC used, for example, by Favrin et al. to study the oligomerization of Aβ_{16-22}.[20] Second, the efficiency of this method is independent of the height of the energy barrier at the transition point. It is therefore possible for the system to move through the conformation space rapidly, without having to wait for the rare fluctuations to occur. In the systems discussed here, it is not rare to generate events with RMSD larger than 1 Å per atom, which thus move the system from one basin of attraction to another.

Recent comparison with other activated methods have shown that ART is the most efficient activated algorithm for sampling the energy landscape of high-dimensional problems.[21] Moreover, tests on clusters and proteins have demonstrated that ART does not seem to miss any class of event and that those are reversible, that is, if ART finds a path going from minimum A to minimum B, then it will also be able to find the reverse path, from B to A. This is important because these two properties ensure that ART is ergodic.

Since events are accepted based on the conformation energy at the local minimum, the entropy is not included in the accept/reject criterion. This implies that the Metropolis temperature cannot be directly connected to a real temperature and causes proteins to remain relatively compact even at high T. While this can sometimes be an inconvenience, it facilitates conformational sampling around the native or the aggregated states even at high

temperature, where standard methods would tend to unravel everything. It is not necessary, for example, to include an additional term in the energy or to place the peptides inside a sphere to keep them together. Moreover, by not fully including entropic contributions, ART can sample a wider range of trajectories. For example, while we were able to identify three different folding mechanisms for a 16-residue β-hairpin, all other methods could only recover one of these, depending on the simulation details.

Another limitation of ART is that it is not dynamical in nature: formally, there is no reason to suppose that the generated trajectories have any relation with the real folding or aggregation process. However, since each ART-generated event connects two minima via a shared transition point, all simulated trajectories are physically possible. Moreover, in numerous comparisons with MD, we have found that ART-generated pathways are in close agreement with dynamical trajectories. For example, the three folding pathways predicted for a β-hairpin using ART[22] were recovered by extensive all-atom MD on a related peptide.[23] In addition, recent studies suggest that the structure of the protein energy landscape is such that folding trajectories, irrespective of their dynamics, should be qualitatively the same.[24,25]

2.2. Protein and Energy Model. The atomic interactions are described using the optimized potential for efficient peptide-structure prediction (OPEP), which was trained on the structures of six polypeptides in solution but not Aβ.[26,27] This potential is based on a simplified off-lattice protein chain representation with all backbone atoms included (i.e., N, H, C_α, C, and O). Each amino acid side chain type is modeled by one bead with a van der Waals radius and geometrical parameters with respect to the backbone (Figure 1B) in agreement with the analysis of side chains in high-resolution protein structures.[27]

The OPEP energy function is expressed as a function of four types of interaction: (i) harmonic potentials to maintain bond lengths, bond angles, improper angles of side chains, and peptide bonds (ω) near their equilibrium values; (ii) excluded-volume potentials between all particles, with the exception of side chain−side chain interactions; (iii) backbone two-body and four-body (cooperative) hydrogen-bonding interactions between any carbonyl oxygen and amide nitrogen separated at least by four amino acids to stabilize possible secondary structures; (iv) a 12−6 potential between side chains if the interaction is hydrophobic in character or results from two opposite charged residues and a 6-repulsive potential otherwise.[26,22]

No type of interactions plays a crucial role in OPEP. Rather, it is the subtle balance between the long-range side-chain interactions (we use a 20 amino acid alphabet) and the main-chain hydrogen-bonding interactions (both short- and long-range in character) that stabilizes the native structures of small peptides in solution. This runs in contrast with the potential that has been used in DMD simulations of polyalanines, where the energy associated with the hydrogen bonds (H-bonds) is certainly not physical.[28]

Because of the coarse-grained nature of the side chains, OPEP cannot capture the full complexity of hydrophobic and electrostatic interactions between all-atom side chains.[20,29−32] In addition, OPEP is based on an implicit solvent representation and thus does not take into account H-bonds between the proteins and the solvent like other force fields.[33,34] Nevertheless, the OPEP force field has been used with ART and other Monte Carlo-based methods to predict the native structures of small proteins in solution with three α-helices,[29] β-sheets,[22] or α/β secondary structures.[35] In addition, the ART−OPEP folding trajectories of a β-hairpin model generate mechanisms similar to those described by standard protocols using all-atom models.[22]

2.3. Simulation Details. The N and C termini of each amyloid-forming chain is blocked with acetyl and amide groups, respectively. Each oligomer was typically subjected to 20−40 ART−OPEP simulations. ART was carried out in Cartesian coordinate space, but internal coordinate space can also be used (unpublished results). Each simulation was conducted for 8000−15 000 events starting from various conformations and orientations of the chains within a sphere of diameter 50 Å using different random number seeds. The size of the sphere is not critical since in the absence of inertia, monomers always aggregate due to long-range interactions. The Metropolis temperatures used for the simulations depend on the peptide length and oligomer size and were set between 300 and 600 K. As discussed in the previous section, this temperature is somewhat artificial, and it is adjusted to ensure an efficient sampling of the energy landscape.

To complement ART−OPEP simulations, we have also performed a number of MD simulations in water using the GROMACS program, the GROMOS force field and specific starting points.[36] These all-atom MD simulations were performed with periodic boundary conditions at constant temperature (298 and 330 K) and constant pressure (1 atm) and a time-step of 2 fs, and the particle mesh Ewald method was used with a cutoff distance of 12 Å for the electrostatic interactions.

3. Aggregation Process of Amyloid-Forming Peptides

There have been considerable experimental efforts devoted, in recent years, to determine the detailed atomic structure of amyloid fibrils, as well as the mechanisms and the driving forces for multisheet assembly. Because of experimental limitations, computer simulations provide a much-needed complement to existing experimental studies and offer precise predictions that can serve as a basis for further experimental studies.

3.1. Self-Assembly of Dimers and Trimers. To understand the basic aggregation mechanisms, several recent studies have focused on dimers and trimers of two heptapeptides: Aβ_{16-22} and the GNNQQNY fragment from the yeast prion protein. The aggregation pathways of Aβ_{16-22} were studied by ART−OPEP,[9,10] all-atom implicit solvent MD at high temperature,[30] and all-atom explicit solvent MD at 300 K using constraints between the chain

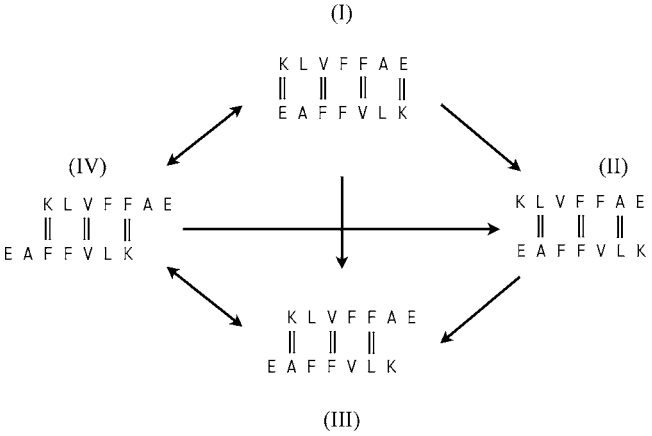

FIGURE 2. Four predicted antiparallel β-sheet registries of the dimer of Aβ_{16-22}. Vertical double lines indicate H-bonds. One way and two-way arrows indicate transitions observed by ART simulations.

centers of mass.[31] The second peptide was studied using implicit solvent replica exchange MD at 330 K.[32] All these simulations converge in demonstrating the richness of the conformational space associated with these small oligomers.

ART−OPEP simulations show that the predicted lowest-energy structure of the dimer and trimer of Aβ_{16-22} is antiparallel in character and superimposes onto the in-fibril conformation with a precision of about 1 Å rms deviation.[9,10] But these simulations offer a much richer picture: a number of ordered β-sheets with out-of-register antiparallel or parallel character are also found with OPEP energies only slightly above the in-register antiparallel β-sheets. This ART-generated distribution of populated states for the dimer is validated by high-temperature MD simulations on Aβ_{16-22} and related peptides, although the structural details for these high-temperature conformations are not provided.[30] Figure 2 summarizes the four predicted antiparallel β-sheet registries for the dimer. Interestingly, the alternation of patterns I and II is necessary to propagate the full fibril structure deduced from NMR solid-state analysis.[14]

The existence of a nonnegligible population of structures with parallel organization in dimers and trimers helps explain the shift from antiparallel to parallel structure observed between Aβ_{16-22} and full-length Aβ's or octanoyl-Aβ_{16-22}[37] (the formula of octanoyl is $CH_3(CH_2)_6$-(COOH)). Since both orientations are found in small fragments, this transition is due to a shift in free energy as peptide length increases (Aβ) or peptide amphiphilicity changes (octanoyl-Aβ_{16-22}).

Similarly, the relation between low-energy in-register and out-of-register antiparallel or mixed parallel−antiparallel β-sheets in ART-generated trajectories for the trimer resembles that provided by replica exchange MD simulations on the yeast prion fragment.[32] The misaligned β-sheets of the Aβ_{16-22} trimer were also found to be stable within 20 ns by all-atom explicit solvent MD simulations.[10] These combined studies demonstrate that trimers can form in-register, out-of register, and mixed alignments with specific populations determined by the solvent conditions, helping understanding of the experimental

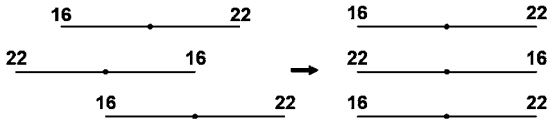

FIGURE 3. Schematic representation of the aggregation of the trimer of Aβ_{16-22}. Convergence toward the native β-sheet registry involves reptation move of the chains. The gray circle represents the position of F19 within each chain. Interchain H-bonds are not shown.

dependency of β-sheet registry on pH conditions. For instance, Petkova et al. found that the Aβ_{11-25} fibrils have distinct H-bond patterns at pH 7.4 and 2.4.[38] Naito et al. found that the fibril structure of the 32-residue human calcitonin shifts from antiparallel β-sheets at pH 4.1 to a mixture of parallel and antiparallel β-sheets at pH 3.3.[39]

While following Aβ_{16-22} dimer formation can provide essential information as to the stability of the various basic structures, the trimer helps us understand the first steps in the oligomeric growth process. Figure 3 offers a schematic description of the aggregation ART trajectories for the trimer of Aβ_{16-22}. We see that even for this short peptide folding proceeds through nonnative alignments of β strands. The transition between off-registry and in-registry β-sheets does not require a transient dissociation of the chains. It constitutes rather a clear reptation move of one chain with respect to another, a mechanism we find independently of the size of the oligomers. The exact energy barriers between misaligned and aligned states are unknown; the time scale for such a reptation move is not in the nanosecond but rather within the microsecond−millisecond range. Interestingly, this reptation mechanism, predicted initially for a β-hairpin,[22] was observed by a recent isotope-edited IR spectroscopy study on the prion fragment PrP$_{109-122}$ at high concentration.[40]

Since the possible number of nonnative β-sheets scales with n^{N-1} (where n is the number of H-bonds within a dimer and N the size of the nucleus) and many of these states should be isoenergetic for oligomers below the critical nucleus size, we believe that nonnative β-sheets represent kinetic traps that contribute to the lag-phase period observed in the kinetics of Aβ_{1-40} fibrillogenesis. These kinetic traps were also discussed in two papers reporting implicit solvent MD of the dimer of Aβ_{16-22} at 498 K[30] and implicit solvent replica exchange MD of the trimer of a yeast prion fragment at 330 K.[32]

3.2. Fibril: Structure and Growth Mechanims. To get a clear understanding of the molecular mechanisms governing fibril assembly at an atomic level, simulations were conducted on distinct polypeptides using different levels of chain representation. Simulations on tetramers with all-atom or six particles per amino acid include the KFFE peptide using ART,[11] the transthyretin protein fragment 105−115 using implicit solvent 2.5 μs MD simulations with chemical shift constraints,[29] and the islet amyloid fragment NFGAIL by explicit solvent 0.6 μs MD simulations.[34] Oligomers with 32 and 96 chains were also studied using DMD simulations and four particles per amino acid.[28,41]

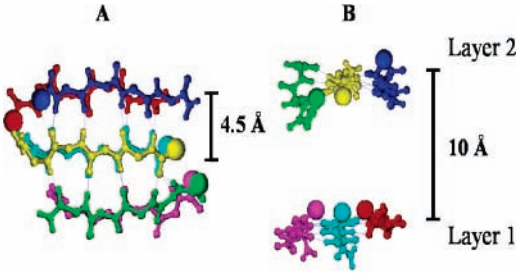

FIGURE 4. Two views of one ART-predicted structure for six chains of KFFE. Panels A and B show the expected meridional and equatorial reflections, respectively. Side chains are omitted for clarity.

Consistent with MD results on KFFE[11] and related peptides,[29,34] ART simulations show that four KFFE peptides are in equilibrium between tetramers with fully antiparallel or mixed parallel-antiparallel β-sheets, mixed trimer−monomer and dimer−dimer conformations.[11] This distribution is also supported by explicit solvent MD simulations of NFGAIL starting from various preformed assemblies.[42] Taken together these results demonstrate that a two-layer β-sheet cannot be formed with only four small chains.

Increasing the number of chains to a minimum number of six peptides, however, changes the structural properties of the possible oligomers qualitatively. Extensive ART−OPEP simulations show that six chains of KFFE self-associate to adopt, with various orientations, three possible distant almost isoenergetic structures.[12] The first one consists of a barrel-like curved single layer, while the two others organize into a double-layer β-sheet assembly with both the meridional 4.75 Å and the equatorial 10 Å distances, or reflections, observed in the diffraction patterns of many amyloid fibers (see Figure 4). The first reflection is associated with the backbone separation within one β-sheet (or layer) and the second with the backbone separation between layers (or protofibrils).

Formation of two protofibrils is independent of the number of chains as long as it is equal to or greater than six; identical formations are obtained for seven (unpublished results) and eight KFFE chains.[13] It is also independent of the details of the force field used and the exact amino acid composition: the cross-β structure was recently observed in all-atom implicit solvent tempering MC simulations of six chains of $A\beta_{16-22}$[20] and in DMD simulations of polyalanines.[28]

The ART-generated assembly process leading to a two-layer KFFE β-sheet is described in Figure 5. Starting from a randomly chosen conformation and orientation of the chains (a), an antiparallel dimer forms (b) and attracts a third chain in a parallel orientation (c). At the same time, the remaining three chains associate into a disordered aggregate, although intermolecular H-bonds form between two chains (c). The first formed antiparallel−parallel trimer helps stabilize the formation of the second trimer (d). Both interpeptide and intrapeptide interactions contribute to the formation of two parallel β-sheets (e). On the basis of these simulations, we suggested that the growth of fibrils made of short peptides follows a bidirectional growth mode with an alternate longitudinal

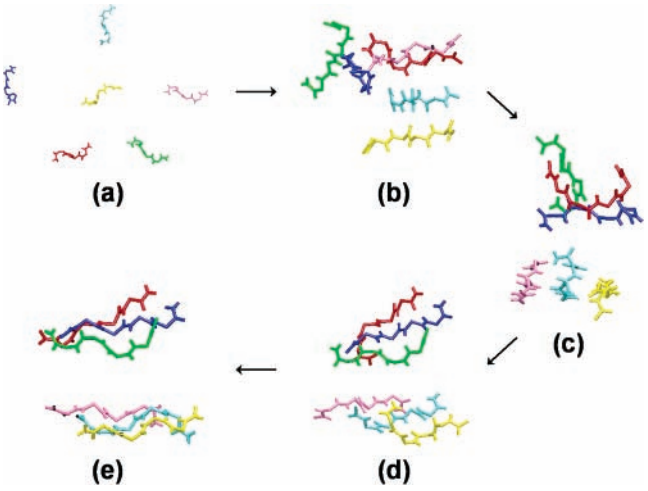

FIGURE 5. Assembly process of six KFFE chains into a two-layer β-sheet. Side chains are not shown.

growth (β-sheet elongation) and lateral growth (association of protofibrils).[12] Such a mechanism, observed in DMD simulations of polyalanines,[28] is consistent, although more precise, with that detected in human amylin by time-lapse atomic force microscopy, where lateral growth of oligomers is followed by longitudinal growth into mature fibrils.[43]

Although six to eight KFFE chains can already generate small protofibrils with the cross-β structure, our simulations reveal a number of competitive structures of increasing complexity with chain number. If, as discussed above, six KFFE chains can form a barrel-like curved single-layer, seven or eight chains are sufficient to produce various types of micelles.[12,13] This finding indicates that full structural order in fibril requires large aggregates and that aggregation involves a variety of distinct oligomeric intermediates, in agreement with experiment.

3.3. Fibril Growth: Driving Forces. Since many amino acid sequences can assemble into an amyloid fiber, given the right experimental conditions, it is important to understand the driving forces promoting this structure. It is well established that the propensity to form fibrils is highly dependent on the pH, ionic strength, and concentration of the solution. There is also strong experimental evidence that aromatic interactions resulting from the phenylalanine and tyrosine rings play a crucial role in amyloid formation.[44,45] For instance, KFFE forms fibrils, but KLLE does not.[15] We found that the variant KPGE forms disordered aggregates,[11] as expected from the β-sheet breaker property of the proline amino acid used for designing anti-amyloid agents.[46] The role of π-stacking in maintaining preformed assemblies has also been documented by explicit solvent all-atom MD simulations of several mutants.[31,42] These aromatic interactions and more generally the hydrophobic interactions are, however, not sufficient. For instance, the peptide Ac−STVIYE-Am, which contains one tyrosine amino acid, has a random coil circular dichroism spectrum.[47] It appears that a delicate balance between hydrophobic forces, Coulombic interactions, and secondary structure propensities is involved in the formation of fibrils [31,42,47,48] and the effects

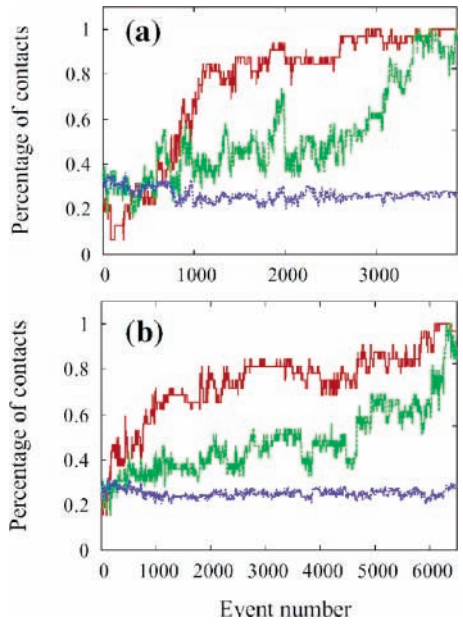

FIGURE 6. Contact evolution as a function of ART events from two simulations leading to a two-layer β-sheet. The percentages of native $C_\alpha - C_\alpha$ (red), native side chain−side chain (green) and total side chain−side chain (blue) contacts are shown.

of mutations on the rates of aggregation of unfolded polypeptide chains can be correlated with changes in simple physicochemical properties.[49]

The driving forces have been studied by ART for six KFFE chains.[12] KFFE is a good model system because it contains two charged side chains (K and E) and two aromatic side chains (F). As seen in Figure 6, the formation of two-layer β-sheets involves three steps. Nonnative side chain electrostatic and hydrophobic interactions bring the peptides together, which allow the native backbone−backbone interactions to start the assembly of β-sheets, although in nonnative β-sheet registries. Once these are formed, the final organization appears to be driven by native side chain−side chain interactions. Simulations on a mutated sequence show that the formation is sequence-specific.[11]

Overall, this ART-derived aggregation picture is consistent with MD simulations on related peptides,[30−32] but our mechanism puts more emphasis on the crucial role of the main chain H-bonds in guiding the peptides to fully ordered aggregates. This role of backbone H-bonds is also confirmed by the destabilizing effect of urea on oligomers.[50]

4. Conclusions

This Account presents a synthesis of our aggregation studies to help in understanding the atomic details of the self-assembly of proteins to form amyloids. Such a knowledge, which complements experimental data (early assemblies are metastable and transient and therefore cannot be easily identified using biophysical methods), would allow one to target the interaction sites between oligomers and current inhibitors (e.g., peptides containing proline or α-aminoisobutyric acid or N-methylation of selective backbone amides) and thus has important implications for the design of improved anti-amyloid agents. The peptides used in ART−OPEP simulations are of different sizes and sequences. We further put our results in the context of current experimental data and other theoretical works.

As is underlined experimentally, there is much variation in the local structure of oligomers as a function of chain length or amino acid sequence. However, simulations on simple models are able to reproduce two important experimental results: the generic cross-β structure with the meridional and equatorial reflections (observed for most amyloids) and the transition through nonnative β-sheets prior to final assembly (observed thus far on a PrP fragment[40]). ART−OPEP simulations also help understand the experimental dependency of β-sheet registry on pH conditions[38,39] and reveal a fibril growth mechanism of short chains that was observed by atomic force spectroscopy.

ART−OPEP simulations demonstrate the existence of thresholds for the formation of the generic cross-β structure. They also emphasize the multiplicity of metastable structures associated with specific oligomeric sizes. Much remains to be done, however, to solve the aggregation processes and the structures of the toxic oligomers associated with Alzheimer's disease. DMD simulations on multimers of $A\beta_{1-40}$[41] and theoretical calculations on the dimer of $A\beta_{10-35}$[51] have recently focused on this aspect. Given the challenges of experimentally characterizing these oligomers, and following on our current studies, it is clear that numerical methods, including ART−OPEP, will continue to play a central role in proposing such structural and dynamical information.

P.D. and N.M. thank the IDRIS and CINES centers in France and the RQCHP center in Quebec for their generous computational support. N.M. is Cottrell Scholar of the Research Corporation and is supported in part by grants from NSERC, FQRNT and the Canada Research Chair program.

References

(1) Kelly, J. F. The alternative conformations of amyloidogenic proteins and their multistep assembly pathways. *Curr. Opin. Struct. Biol.* **1998**, *8*, 101−106.
(2) Dobson, C. M. Protein misfolding diseases: getting out of shape. *Nature* **2002**, *418*, 729−730.
(3) Prusiner, S. B. Prion diseases and the BSE crisis. *Science* **1997**, *278*, 245−251.
(4) Petkova, A. T.; Leapman, R. D.; Guo, Z.; Yau, W. M.; Mattson, M. P.; Tycko, R. Self-propagating, molecular-level polymorphism in Alzheimer's beta-amyloid fibrils. *Science* **2005**, *307*, 262−265.
(5) Nilsson, M. R. Techniques to study amyloid fibril formation in vitro. *Methods* **2004**, *34*, 151−160.
(6) Walsh, D. M.; Klyubin, I.; Fadeeva, J. V.; Cullen, W. K.; Anwyl, R.; Wolfe, M. S.; Rowan, R. J.; Selkoe, D. J. Naturally secreted oligomers of amyloid beta protein potently inhibit hippocampal long-term potentiation in vivo. *Nature* **2002**, *416*, 535−539.
(7) Kayed, R.; Head, E.; Thompson, J. L.; McIntire, T. M.; Milton, S. C.; Cotman, C. W.; Glabe, G. C. Common structure of soluble amyloid oligomers implies common mechanism of pathogenesis. *Science* **2003**, *300*, 486−489.
(8) Bitan, G.; Teplow, D. B. Rapid photochemical cross-linking-a new tool for studies of metastable, amyloidogenic protein assemblies. *Acc. Chem. Res.* **2004**, *37*, 357−364.
(9) Santini, S.; Wei, G. H.; Mousseau, N.; Derreumaux, P. Pathway complexity of Alzheimer's beta-amyloid A β_{16-22} peptide assembly. *Structure* **2004**, *12*, 1245−1255.

(10) Santini, S.; Mousseau, N.; Derreumaux, P. In silico assembly of Alzheimer's Aβ_{16-22} peptide into β-sheets. *J. Am. Chem. Soc.* **2004**, *126*, 11509−11516.
(11) Melquiond, A.; Boucher, G.; Mousseau, N.; Derreumaux, P. Following the aggregation of amyloid-forming peptides by computer simulations. *J. Chem. Phys.* **2005**, *122*, 174904.
(12) Wei, G. H.; Mousseau, N.; Derreumaux, P. Sampling the self-assembly pathways of KFFE hexamers. *Biophys. J.* **2004**, *87*, 3648−3656.
(13) Wei, G.; Mousseau, N.; Derreumaux, P. Assembly dynamics of KFFE octamers. *J. Phys.: Condens. Matter* **2004**, *16*, 5047−5054.
(14) Balbach, J. J.; Ishii, Y.; Antzutkin, O. N.; Leapman, R. D.; Rizzo, N. W.; Dyda, F.; Reed, J.; Tycko, R. Amyloid fibril formation by Abeta 16−22, a seven-residue fragment of the Alzheimer's beta-amyloid peptide, and structural characterization by solid-state NMR. *Biochemistry* **2000**, *39*, 13748−13759.
(15) Tjernberg, L.; Hosia, W.; Bark, N.; Thyberg, J.; Johansson, J. Charge attraction and beta propensity are necessary for amyloid fibril formation from tetrapeptides. *J. Biol. Chem.* **2002**, *277*, 43243−43246.
(16) Xu, Y.; Shen, J.; Luo, X.; Zhu, W.; Chen, K.; Ma, J.; Jiang, H. Conformational transition of amyloid beta-peptide. *Proc. Natl. Acad. Sci. U.S.A.*, in press
(17) Barkema, G. T.; Mousseau, N. Event-based relaxation of continuous disordered systems. *Phys. Rev. Lett.* **1996**, *77*, 4358−4361.
(18) Malek, R.; Mousseau, N. Dynamics of Lennard-Jones clusters: A characterization of the activation-relaxation technique. *Phys. Rev. E* **2000**, *62*, 7723−7728.
(19) Wei, G. H.; Mousseau, N.; Derreumaux, P. Exploring the energy landscape of proteins: a characterization of the activation relaxation technique. *J. Chem. Phys.* **2002**, *117*, 11379−11387.
(20) Favrin, G.; Irback, A.; Mohanty, S. Oligomerization of amyloid Aβ16−22 peptides using hydrogen bonds and hydrophobicity forces. *Biophys. J.* **2004**, *87*, 3657−3664.
(21) Olsen, R. A.; Kroes, G. J.; Henkelman, G.; Arnaldsson, A.; Jonsson, H. Comparison of methods for finding saddle points without knowledge of the final states. *J. Chem. Phys.* **2004**, *121*, 9776−9792.
(22) Wei, G.; Mousseau, N.; Derreumaux, P. Complex folding pathways in a β-hairpin. *Proteins* **2004**, *56*, 464−474.
(23) Ikeda, K.; Higo, J. Free-energy landscape of a chameleon sequence in explicit water and its inherent a/b bifacial property. *Protein Sci.* **2003**, *12*, 2542−2548.
(24) Rao, F.; Caflisch, A. The protein folding network. *J. Mol. Biol.* **2004**, *342*, 299−306.
(25) Mousseau, N.; Derreumaux, P.; Gilbert, G. Navigation and analysis of the energy landscape of small proteins using the activation-relaxation technique. *Phys. Biol.*, in press.
(26) Derreumaux, P. From polypeptide sequences to structures using Monte Carlo simulations and an optimized potential. *J. Chem. Phys.* **1999**, *111*, 2301−2310.
(27) Derreumaux, P. Generating ensemble averages for small proteins from extended conformations by Monte Carlo simulations. *Phys. Rev. Lett.* **2000**, *85*, 206−209.
(28) Nguyen, N. D.; Hall, C. K. Molecular dynamics simulations of spontaneous fibril formation by random-coil peptides. *Proc. Natl. Acad. Sci. U.S.A.* **2004**, *101*, 16180−16185.
(29) Paci, E.; Gsponer, J.; Salvatella, X.; Vendruscolo, M. Molecular dynamics studies of the process of amyloid aggregation of peptide fragments of transthyretin. *J. Mol. Biol.* **2004**, *340*, 555−569.
(30) Hwang, W.; Zhang, S.; Kamm, R. D.; Karplus, M. Kinetic control of dimer structure formation in amyloid fibrillogenesis. *Proc. Natl. Acad. Sci. U.S.A.* **2004**, *101*, 12916−12921.
(31) Klimov, D. K.; Thirumalai, D. Dissecting the assembly of Abeta-(16−22) amyloid peptides into antiparallel beta sheets. *Structure* **2003**, *11*, 295−307.
(32) Gsponer, J.; Haberthur, U.; Caflisch, A. The role of side-chain interactions in the early steps of aggregation: Molecular dynamics simulations of an amyloid-forming peptide from the yeast prion Sup35. *Proc. Natl. Acad. Sci. U.S.A.* **2003**, *100*, 5154−5159.
(33) Ma, B.; Nussinov, R. Stabilities and conformations of Alzheimer's beta-amyloid peptide oligomers (Aβ_{16-22}, Aβ_{16-35}, and Aβ_{10-35}): sequence effects. *Proc. Natl. Acad. Sci. U.S.A.* **2002**, *99*, 14126−14131.
(34) Wu, C.; Lei, H.; Duan, Y. The role of PHE in the formation of well-ordered oligomers of amyloidogenic hexapeptide (NFGAIL) observed in molecular dynamics simulations with explicit solvent. *Biophys. J.* **2005**, *88*, 2897−2906.
(35) Floquet, N.; Pasco, S.; Ramont, L.; Derreumaux, P.; Laronze, J.-Y.; Nuzillard, J.-M.; Maquart, F. X.; Alix, A. J. P.; Monboisse, J.-C. The anti-tumor properties of the α3(IV) 185−203 peptide from the NC1 domain of type IV collagen (Tumstatin) are conformation-dependent. *J. Biol. Chem.* **2004**, *279*, 2091−2100.
(36) Berendsen, H. J. C.; van der Spoel, D.; van Drunen, R. GROMACS: A message-passing parallel molecular dynamics implementation. *Comput. Phys. Commun.* **1995**, *91*, 43−56.
(37) Gordon, D. J.; Balbach, J. J.; Tycko, R.; Meredith, S. C. Increasing the amphiphilicity of an amyloidogenic peptide changes the beta-sheet structure in the fibrils from antiparallel to parallel. *Biophys. J.* **2004**, *86*, 428−434.
(38) Petkova, A. T.; Buntkowsky, G.; Dyda, F.; Leapman, R. D., Yau, W. M.; Tycko, R. Solid-state NMR reveals a pH-dependent antiparallel beta-sheet registry in fibrils formed by a beta-amyloid peptide. *J. Mol. Biol.* **2004**, *335*, 247−260.
(39) Naito, A.; Kamihira, M.; Inoue, R.; Saito, H. Structural diversity of amyloid fibril formed in human calcitonin as revealed by site-directed 13C solid-state NMR spectroscopy. *Magn. Reson. Chem.* **2004**, *42*, 247−257.
(40) Silva, R. A.; Barber-Armstrong, W.; Decatur, S. M. The organization and assembly of a β-sheet formed by a prion peptide in solution: an isotope-edited FTIR study. *J. Am. Chem. Soc.* **2003**, *125*, 13674−13675.
(41) Urbanc, B.; Cruz, L.; Yun, S.; Buldyrev, S. V., Bitan, G.; Teplow, D. B.; Stanley, H. E. In silico study of amyloid beta-protein folding and oligomerization. *Proc. Natl. Acad. Sci. U.S.A.* **2004**, *101*, 17345−17350.
(42) Zanuy, D.; Ma, B.; Nussinov, R. Short peptide amyloid organization: stabilities and conformations of the islet amyloid peptide NFGAIL. *Biophys. J.* **2003**, *84*, 1884−1894.
(43) Green, J. D.; Goldsbury, C.; Kistler, J.; Cooper, G. J.; Aebi, U. Human amylin oligomer growth and fibril elongation define two distinct phases in amyloid formation. *J. Biol. Chem.* **2004**, *279*, 12206−12212.
(44) Gazit, E. A possible role for pi-stacking in the self-assembly of amyloid fibrils. *FASEB J.* **2002**, *16*, 77−83.
(45) Tracz, S. M.; Abedini, A.; Driscoll, M.; Raleigh, D. P. Role of aromatic interactions in amyloid formation by peptides derived from human Amylin. *Biochemistry* **2004**, *43*, 15901−15908.
(46) Permanne, B.; Adessi, C.; Saborio, G. P.; Fraga, S.; Frossard, M. J.; Van Dorpe, J.; Dewachter, I.; Banks, W. A.; Van Leuven, F.; Soto, C. Reduction of amyloid load and cerebral damage in a transgenic mouse model of Alzheimer's disease by treatment with a beta-sheet breaker peptide. *FASEB J.* **2002**, *16*, 860−862.
(47) Lopez De La Paz, M.; Goldie, K.; Zurdo, J.; Lacroix, E.; Dobson, C. M.; Hoenger, A.; Serrano, L. De novo designed peptide-based amyloid fibrils. *Proc. Natl. Acad. Sci. U.S.A.* **2002**, *99*, 16052−16057.
(48) Fernandez-Escamilla, A. M.; Rousseau, F.; Schymkowitz, J.; Serrano, L. Prediction of sequence-dependent and mutational effects on the aggregation of peptides and proteins. *Nat. Biotechnol.* **2004**, *22*, 1302−1306.
(49) Chiti, F.; Stefani, M.; Taddei, N.; Ramponi, G.; Dobson, C. M. Rationalization of the effects of mutations on peptide and protein aggregation rates. *Nature* **2003**, *424*, 805−808.
(50) Klimov, D. K.; Straub, J. E.; Thirumalai, D. Aqueous urea solution destabilizes Aβ(16−22) oligomers. *Proc. Natl. Acad. Sci. U.S.A.* **2004**, *101*, 14760−14765.
(51) Tarus, B.; Straub, J. E.; Thirumalai, D. Probing the initial stage of aggregation of the Aβ(10−35)-protein: assessing the propensity for peptide dimerization. *J. Mol. Biol.* **2005**, *345*, 1141−1156.

AR050045A